Efficient algorithms for mathematical morphology based on chamfer distances

P.F.M. Nacken

Department of Operations Research, Statistics, and System Theory

Report BS-R9308 April 1993

CWI is the National Research Institute for Mathematics and Computer Science. CWI is part of the Stichting Mathematisch Centrum (SMC), the Dutch foundation for promotion of mathematics and computer science and their applications. SMC is sponsored by the Netherlands Organization for Scientific Research (NWO). CWI is a member of ERCIM, the European Research Consortium for Informatics and Mathematics.

P.O. Box 4079, 1009 AB Amsterdam (NL)
Kruislaan 413, 1098 SJ Amsterdam (NL)
Telephone +31 20 592 9333
Telefax +31 20 592 4199

Efficient Algorithms for Mathematical Morphology Based on Chamfer Distances

P.F.M. Nacken

Institute for Perception TNO
Kampweg 5, 3769 DE Soesterberg, The Netherlands

Abstract

This paper describes a number of efficient algorithms for morphological operations which use discs defined by chamfer distances as structuring elements. It presents an extension to previous work on extending metrics (such as the p-q-metrics). Theoretical results and algorithms are presented for the 5-7-11-metric, which is not extending. This metric approximates the Euclidean metric close enough for most practical situations. The algorithms are based on an analysis of the structure of shortest paths in the 5-7-11-metric and of the set of values this metric can assume. Efficient algorithms are presented for the medial axis and the opening transform. The opening transform algorithm is two orders of magnitude faster than a more straightforward algorithm.

1991 Mathematics Subject Classification: 68U10, 51K99
Keywords & Phrases: mathematical morphology, chamfer metrics, algorithms.

Note: This research was supported by the Foundation for Computer Science in the Netherlands (SION) with financial support from the Netherlands Organization for Scientific Research (NWO). This research was part of a project in which the TNO Institute for Perception (Kampweg 5, 3769 DE Soesterberg, The Netherlands), the Centre for Mathematics and Computer Science (Kruislaan 413, 1098 SJ Amsterdam, The Netherlands) and the Faculty of Mathematics and Computer Science of the University of Amsterdam (Kruislaan 403, 1098 SJ Amsterdam, The Netherlands) cooperate.

1. Introduction

Mathematical morphology [7, 13] is an approach to image processing which is based on set theoretic notions such as inclusion and intersection. Recently, mathematical morphology has been extended to grey level images [13] and even complete lattices [12, 4], but originally mathematical morphology dealt with binary images. Mathematical morphology models binary images as sets, by considering the foreground pixels as a subset of the image plane. The image is analyzed by inspecting the containment or intersection relations of the image with translates of some set B, the structuring element.

When mathematical morphology is applied to images defined on the real plane, one often uses discs as structuring elements. This is a suitable choice, because it makes morphological operators rotation invariant, and because it allows for the interpretation of the results in terms of the natural metric for the image plane. Because discs are defined by a metric, it is possible to express much of the theory of morphological operators based on circular structuring elements in terms of metrics.

Report BS-R9308
ISSN 0924-0659
CWI
P.O. Box 4079, 1009 AB Amsterdam, The Netherlands

In this approach, the notions of distance transformations and reconstructions occur in a natural way.

In practice, images are not defined on the real plane, but on (some subset of) the square grid $\mathbb{Z}^2$. On this grid, chamfer metrics [2] can be defined by setting the distance between pairs of neighboring points, and providing a rule for determining the distance between any pair of points from the distances between neighboring points. The definition of chamfer metrics is presented in the next section. The accuracy of a chamfer metric (compared with the Euclidean metric) can be improved by increasing the number of point pairs for which a prefixed distance is given. In typical cases, the distance of each point to eight other points is given, yielding the so-called p-q-metrics, or the distance to 16 other points is given, yielding the so-called p-q-r-metrics.

Chamfer metrics can be used as accurate approximations to the Euclidean metric, at the same time allowing for efficient computations. In this paper, the metric approach to mathematical morphology will be combined with chamfer metrics in order to define the medial axis, opening transform and pattern spectrum associated with chamfer metrics. Efficient algorithms for these operations will be described.

The medial axis algorithm is different for p-q-metrics, such as the 3-4-metric or the 5-7-metric, and p-q-r-metrics such as the 5-7-11-metric. The author has described the algorithm for p-q-metrics in a previous paper [10]. This paper presents a medial axis algorithm for the 5-7-11-metric. The algorithm for p-q-metrics is presented in this paper for the sake of completeness, and in order to be able to point out the differences with the 5-7-11 metric.

The organization of the rest of the paper is as follows. The next section describes a number of notions from mathematical morphology and chamfer metrics. The tools presented in this section are used in section 3 to derive the medial axis algorithm for the p-q-metric, and in section 4 to present the medial axis algorithm for the 5-7-11-metric. In section 5, algorithms for the opening transform and pattern spectrum are derived, which use the medial axis algorithms derived in the previous sections. The last section sums up the conclusions of this paper.

2. Chamfer Metrics and Mathematical Morphology

In this section, we present the definitions discrete metrics and chamfer metrics and list some of their properties. For a proof of these properties, the reader is referred to a previous paper [10]. We also present some definitions and results on mathematical morphology, in particular the definitions of the medial axis. We will write D for the range $\{d(x,y) \mid x,y \in E\}$ of a metric d on a set E.

1 Definition *A metric d on a set E is called a discrete metric if its range $D = \{d(x,y) \mid x,y \in E\}$ contains no limit points.*

For a metric d, the closed sphere $\overline{B}(x,r)$ with center $x \in E$ and radius $r \in D$ is defined by

$$\overline{B}(x,r) = \{y \in E \mid d(x,y) \leq r\}.$$

One can associate two types of distance transforms with a given discrete metric.

2 Definition *Let d be a discrete metric on E and let D be its range. The external distance transform ρ_X^{ext} is the function $E \to D$ defined by*

$$\rho_X^{\text{ext}}(x) = \min\{d(x,y) \mid y \in X^C\}.$$

3 Definition *Let d be a discrete metric on E and let D be its range. The internal distance transform ρ_X^{int} is the function $X \to D$ defined by*

$$\rho_X^{\text{int}}(x) = \max\{r \in D \mid \overline{B}(x,r) \subseteq X\}.$$

Because D has no limit points, the equality

$$\rho_X^{\text{int}}(x) = \max\{r \in D \mid r < \rho_X^{\text{ext}}(x)\}$$

holds. This equality enables us to compute the internal distance transform from the external one when D is known [10]. In the literature, the external distance transform is used most frequently. In this paper, the internal distance transform is most important, so from now on we will write ρ for the internal distance transform.

A notion closely related to the distance transform is the (closed sphere) reconstruction.

4 Definition *Let d be a discrete metric on E and let D be its range. Let f be a function from a bounded subset X of E to D. The reconstruction $R(f)$ of f is defined as the set*

$$R(f) = \bigcup_{x \in X} \overline{B}(x, f(x)).$$

This definition suggests that a reconstruction can be computed by a simple algorithm. A set is initialized to be empty, and the sphere $\overline{B}(x, f(x))$ is added to it for each $x \in X$. Note that for every bounded set X the relation $X = R(\rho_X^{\text{int}})$ holds.

We will now present the definition of the medial axis [13] and its relation to metrics. From the definition of the internal distance transform, it can easily be deduced that a sphere $\overline{B}(x,r)$ with center $x \in E$ and radius $r \in D$ is included in a set X if and only if $r \leq \rho(x)$. The largest sphere with center x which is contained in X is therefore $\overline{B}(x, \rho(x))$.

5 Definition *Let X be a bounded subset of E and let d be a discrete metric. The medial axis M_X of X is the locus of the centers of maximal spheres in X, i.e. $x \in M_X$ if and only if there is an $r \in D$ such that*

$$\overline{B}(x,r) \subseteq \overline{B}(x',r') \subseteq X \Rightarrow x' = x, r' = r.$$

It can readily be seen that $x \in M_X$ if and only if there is no $y \in X$ such that $y \neq x$ and $\overline{B}(x, \rho(x)) \subseteq \overline{B}(y, \rho(y))$. This property will be used throughout the next sections.

The homotopy of the medial axis of a set X is in general different from the homotopy of the original set. A thin subset of X which has the same homotopy as X and lies in some sense "in the middle" of X is often called a skeleton. The medial axis, skeletons and their relations have been investigated extensively in the past [1, 3, 8, 9, 10, 11, 13].

A particular class of discrete metrics is formed by chamfer metrics [2]. Chamfer metrics were originally defined by Borgefors. In this paper, we restrict ourselves to chamfer metrics on the square grid $\mathbb{Z}^2$. The first step in the construction of a chamfer metric is the selection of a set of so-called prime vectors $\{v_1, \ldots, v_k\}$. Although not necessary from a theoretical point of view [10], it is common to choose a set of prime vectors which is invariant under the symmetry group D_4 of the square grid; D_4 consists of 4 rotations (including the identity) and 4 reflections in horizontal, vertical and diagonal lines. Common choices are to use the four vectors of the form $(\pm 1, 0)$ or $(0, \pm 1)$, the eight vectors of the form $(\pm 1, 0)$, $(0, \pm 1)$ or $(\pm 1, \pm 1)$ or the sixteen vectors of the form $(\pm 1, 0)$, $(0, \pm 1)$, $(\pm 1, \pm 1)$, $(\pm 1, \pm 2)$ or $(\pm 2, \pm 1)$. These sets of prime vectors correspond to the 4-neighborhood, the 8-neighborhood and the neighborhood containing the 8-neighbors and the pixels at a knights mover from the center, respectively.

The next step is the assignment of a weight $l(v_i)$ to each prime vector. These weights are positive numbers; in this paper, we use integers only. The weights are chosen such that they are invariant under the symmetry group D_4 of the grid. Therefore, if eight prime vectors are chosen as mentioned above, the four vectors $(\pm 1, 0)$ and $(0, \pm 1)$ must have the same weight p, and the four vectors $(\pm 1, \pm 1)$ must also have the same weight q. If sixteen prime vectors are chosen as mentioned above, the eight vectors $(\pm 1, \pm 2)$ and $(\pm 2, \pm 1)$ must have the same weight r. The resulting chamfer metrics will be called p-q-metrics and p-q-r-metrics, respectively.

The chamfer metric corresponding to a given set of prime vectors and their weights can now be defined as follows.

6 Definition *Let $\{v_1, \ldots, v_k\}$ be a set of prime vectors, invariant under D_4 and let $l(v_i)$ be their weights, also invariant under D_4. The chamfer metric d on $\mathbb{Z}^2$ is defined by*

$$d(x, y) = \min\{\sum_i n_i l(v_i) \mid n_i \in \mathbb{N}, \sum_i n_i v_i = y - x\}.$$

It is not hard to see that this definition is equivalent to the more common definition using paths, which one often encounters in the literature.

Suppose that no two prime vectors point in the same direction. Then the prime vectors can be ordered clockwise according to their direction. Two prime vectors will be called *adjacent* if they are adjacent in this ordering. An equivalent definition is the following: two prime vectors v_1 and v_2 are adjacent if the only prime vectors in $\{\lambda_1 v_1 + \lambda_2 v_2 \mid \lambda_1, \lambda_2 \in \mathbb{R}, \lambda_1, \lambda_2 \geq 0\}$ are v_1 and v_2. Let $\hat{v}_i = v_i / l(v_i)$ be the so called normalized prime vectors. These prime vectors will in general not be elements of the discrete grid $\mathbb{Z}^2$. We will often use the following theorem [10]:

7 Theorem *Suppose that a set $\{v_1, \ldots, v_k\}$ with weights $l(v_i)$ satisfies the following properties:*
(1) If $v_1 = (x_1, y_1)$ and $v_2 = (x_2, y_2)$ are adjacent prime vectors, then $x_1 y_2 - x_2 y_1 = \pm 1$.
(2) The normalized prime vectors $v_i / l(v_i)$ are the corners of a convex polygon.
Then each vector x of the square grid can be written in a unique way in the form $n_1 v_1 + n_2 v_2$, where v_1 and v_2 are adjacent prime vectors, n_1 and n_2 are nonnegative integers and $d(x, 0) = n_1 l(v_1) + n_2 l(v_2)$.

All chamfer metrics one usually comes across satisfy these conditions. If one finds a way of writing a vector $y - x$ as $n_1 v_1 + n_2 v_2$ where n_1, n_2, v_1 and v_2 are as described above, it follows from the uniqueness of this expression that $d(x, y) = n_1 l(v_1) + n_2 l(v_2)$.

Note that, in general, not all integers occur in the range $D = \{d(x, 0) \mid x \in \mathbb{Z}^2\}$. It can be shown [10] that if the weights of adjacent prime vectors have greatest common divisor 1, the range contains all but a finite number of natural numbers. The ranges of a p-q-metric and a p-q-r-metric will sometimes be written as D_{p-q} and D_{p-q-r}, respectively.

3. The Medial Axis for the p-q-Metric

In this section, we present the medial axis algorithm for p-q-metrics. This algorithm uses a no-upstream condition for the internal distance transform which is analogous to the no-upstream condition which holds for the medial axis in $\mathbb{R}^2$ [8]. Recall that, if X is some open subset of $\mathbb{R}^2$, its distance transform ρ is the function from $\mathbb{R}^2$ to $\mathbb{R}$ defined by $\rho(x) = \inf\{d(x, y) \mid y \in X^C\}$. A point $x \in X$ is a medial axis point if and only if there is no $y \neq x$ such that $\rho(y) = \rho(x) + d(x, y)$.

The algorithm presented in this section for p-q-metrics uses the fact that these metrics are extending:

8 Definition *A metric d on a set E with range D is called extending if for each $x, y \in E$ and $r \in D$ there is a $z \in E$ such that $d(x,y) + d(y,z) = d(x,z)$ and $d(y,z) = r$.*

The Euclidean metric is extending. Given x, y and r, the point z as described in the definition can be constructed using simple geometry: it is one of the intersections of the line xy with the circle with center y and radius r. Of the two intersection points, the one must be chosen for which y lie between x and z.

All p-q-metrics are extending as well. This can be shown by constructing a point z, as we did in the previous paragraph for the Euclidean metric. Let x and y be two points in $\mathbb{Z}^2$ and let $r \in D_{p-q}$. The vector $y-x$ can be written in the form $n_1 v_1 + n_2 v_2$, where v_1 and v_2 are adjacent prime vectors and n_1 and n_2 are non-negative integers. Without loss of generality, it can be assumed that $l(v_1) = p$ and $l(v_2) = q$. As $r \in D_{p-q}$, r can be written as $m_1 p + m_2 q$, where m_1 and m_2 are nonnegative integers. We can take $z = y + m_1 v_1 + m_2 v_2$. Then $z - y = m_1 v_1 + m_2 v_2$, so $d(y,z) = m_1 p + m_2 q = r$. Moreover, $z - x = (n_1 + m_1)v_1 + (n_2 + m_2)v_2$, so $d(x,z) = (m_1 + n_1)p + (m_2 + n_2)q = d(x,y) + d(y,z)$.

The following theorem presents the no-upstream condition for medial axis points for extending metrics.

9 Theorem *Let d be an extending metric on $\mathbb{Z}^2$. Let X be a bounded subset of $\mathbb{Z}^2$. A point $x \in X$ is the center of a maximal sphere if and only if there is no $y \neq x$ such that $\rho(y) \geq \rho(x) + d(x,y)$ ("x has no upstream").*

PROOF. 'only if': suppose that there exists an $y \neq x$ such that $\rho(y) \geq \rho(x) + d(x,y)$. In that case every $z \in \overline{B}(x, \rho(x))$ satisfies

$$d(z,y) \leq d(z,x) + d(x,y) \leq \rho(x) + d(x,y) \leq \rho(y).$$

Therefore $\overline{B}(y, \rho(x))$ is a sphere containing $\overline{B}(x, \rho(x))$ and contained in X. Therefore, x is not the center of a maximal sphere.

'if': Suppose x is not the center of a maximal sphere. Then the sphere with center x and radius $\rho(x)$ must be contained in a closed sphere with center $y \neq x$ and radius $\rho(y)$. Let z be a point such that $d(y,x) + d(x,z) = d(y,z)$ and $d(x,z) = \rho(x)$. Such a points exists because d is extending. From $z \in \overline{B}(x, \rho(x)) \subseteq \overline{B}(y, \rho(y))$ it follows that $d(z,y) \leq \rho(y)$. From these relations it can be deduced that

$$\rho(y) - \rho(x) \geq d(z,y) - \rho(x) = d(z,y) - d(x,z) = d(x,y).$$

∎

This theorem provides a characterization of the medial axis points, but it cannot be used for the construction of an efficient algorithm: in order to determine whether x is a medial axis point of X, all points y must be inspected. In the case of the chamfer metric, the search can be limited to the neighbors of x.

10 Theorem *Let X be a bounded subset of $\mathbb{Z}^2$, provided with the p-q-metric and let $x \in X$. If there is a point y such that $\rho(y) \geq \rho(x) + d(x,y)$, then there is also an 8-neighbor y' of x satisfying $\rho(x) + d(x,y')$.*

PROOF. Let x and y be points as described in the theorem. Then

$$\overline{B}(x, \rho(x)) \subseteq \overline{B}(y, \rho(y)) \subseteq X.$$

There is a pair of adjacent prime vectors v_1 and v_2 such that $x - y = n_1 v_1 + n_2 v_2$ and n_1 and n_2 are non-negative. Without loss of generality, it can be assumed that $n_1 > 0$. We can now take

$y' = x - v_1$. This implies $d(x,y) = d(x,y') + d(y',y)$ and y' is an 8-neighbor of x. It is now sufficient to prove that

$$\overline{B}(x,\rho(x)) \subseteq \overline{B}(y',\rho(x) + d(x,y')) \subseteq \overline{B}(y,\rho(y)).$$

The first inclusion follows from

$$d(x,p) \leq \rho(x) \Rightarrow d(y',p) \leq d(y',x) + d(x,p) \leq d(y',x) + \rho(x).$$

The second inclusion follows from:

$$d(y',p) \leq \rho(x) + d(x,y') \Rightarrow$$
$$d(y,p) \leq d(y,y') + d(y',p) \leq d(x,y') + d(y',y) + \rho(x) = d(x,y) + \rho(x) \leq \rho(y).$$

∎

This theorem suggests the following algorithm for the computation of the medial axis in the p-q-metric.

11 Algorithm *The computation of the medial axis of a bounded subset X of $\mathbb{Z}^2$ with respect to the p-q-metric.*
(1) Compute the external distance transform of X.
(2) Compute the internal distance transform ρ of X from the external one.
(3) Mark all points x having no 8-neighbor y with $\rho(y) \geq \rho(x) + d(x,y)$.

This algorithm requires four image scans, and local computation only. It is possible to perform steps (2) and (3) in a single scan, but this makes the local operation to be performed in this step much more complicated, so this is not a good approach.

4. The Medial Axis for the 5-7-11-Metric.

The 5-7-11 chamfer metric can approximate the Euclidean metric more accurately than any p-q-metric [14]. The relative error of the 5-7-11-metric with respect to the Euclidean metric is 1.79%, while the relative error of any p-q-metric is at least 3.96%. This implies that the error made when measuring an object of diameter 50 is in the order of a single pixel when the 5-7-11-metric is used. Therefore, the accuracy of the 5-7-11-metric is sufficient in most practical situations.

On the other hand, the algorithms for the 5-7-11-metric are more complicated than those for the 5-7-metric. The medial axis algorithm described in the previous section can not be used, because the 5-7-11-metric is not extending. This can be seen from the example in figure 1. The small sphere of radius 5 is contained in the larger one of radius 11, but the distance of their centers is 7, while the difference of their radii is only 6. This sections presents an algorithm which is suitable for the 5-7-11-metric.

For the 5-7-11-metric, there are three types of prime vectors: those of the form $(\pm 1, 0)$ or $(0, \pm 1)$ with weight 5, those of the form $(\pm 1, \pm 1)$ with weight 7 and those of the form $(\pm 1, \pm 2)$ or $(\pm 2, \pm 1)$ with weight 11. We will say that these vectors are of type 5, type 7 or type 11, respectively. Each vector of type 11 is adjacent to a vector of type 5 and a vector of type 7, but no pair of vectors of type 5 and type 7 are adjacent (see figure 2). As a consequence, each shortest path between two points contains either vectors of type 5 and type 11, vectors of type 7 and type 11 or vectors of a single type. The range D_{5-7-11} of the 5-7-11-metric consists of the points which can be written as $5p + 11q$ or $7p + 11q$, for nonnegative p and q. Note that integers larger that 59 can be written in both forms (see [10] for a discussion of the structure of D).

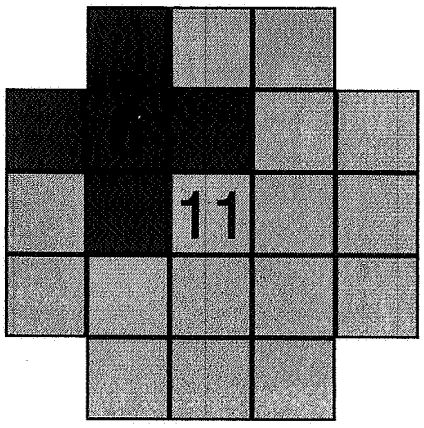

Figure 1: An example showing that the no-upstream criterion for the medial axis can not be applied to the 5-7-11 metric.

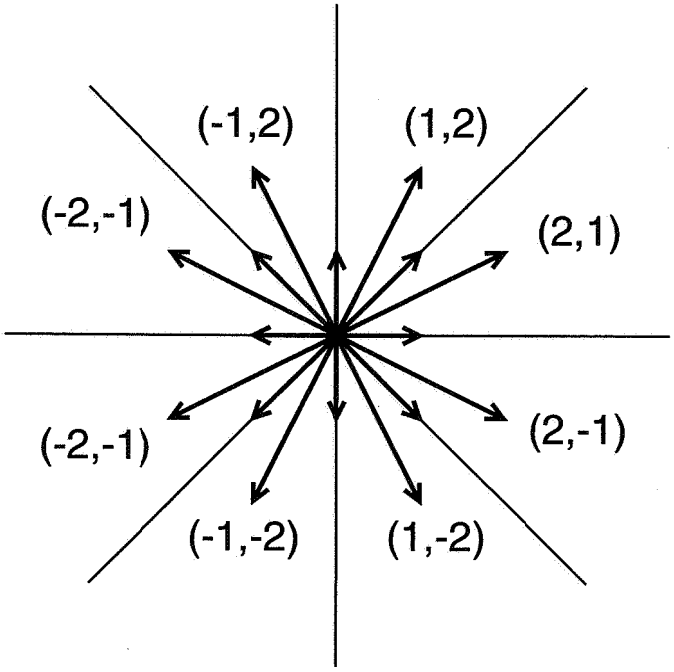

Figure 2: Horizontal, vertical and diagonal vectors partition the plane in eight parts, which can be labeled according the vector of type 11 they contain.

In order to determine whether a point x of an object X is a medial axis point, two cases, depending on the value of $\rho(x)$, must be discerned. These cases are: (1) $\rho(x)$ is an element of both $5\mathbb{N}+11\mathbb{N}$ and $7\mathbb{N}+11\mathbb{N}$; (2) $\rho(x)$ is an element of only one of the sets $5\mathbb{N}+11\mathbb{N}$ and $7\mathbb{N}+11\mathbb{N}$.

The first case is simple. In fact, it is completely analogous to the situation described in the previous section for extending metrics.

12 Theorem *Let X be a bounded subset of $\mathbb{Z}^2$. Suppose that $\rho(x)$ is an element of both $5\mathbb{N}+11\mathbb{N}$ and $7\mathbb{N}+11\mathbb{N}$. Then x is a medial axis point if and only if there is no point y such that $\rho(y) \geq \rho(y) + d(x,y)$.*

PROOF. 'only if': this part of the proof is equal to the corresponding part of the proof in the

previous section. Suppose that there exists a $y \neq x$ such that $\rho(y) \geq \rho(x) + d(x,y)$. Then every $z \in \overline{B}(x, \rho(x))$ satisfies

$$d(z,y) \leq d(z,x) + d(x,y) \leq \rho(x) + d(x,y) \leq \rho(y).$$

Therefore $\overline{B}(y, \rho(y))$ is a sphere containing $\overline{B}(x, \rho(x))$ and contained in X. Consequently, x is not the center of a maximal sphere.

'if': Suppose that x is not the center of a maximal sphere. Then there is a point y such that $\overline{B}(x, \rho(x))$ is contained in $\overline{B}(y, \rho(y))$. Suppose that $x - y = n_1 v_1 + n_2 v_2$ for adjacent prime vectors v_1 and v_2 and nonnegative n_1, n_2. The prime vectors are either of type 5 and 11 or of type 7 and 11. In both cases, $\rho(x)$ can be written in the form $m_1 l(v_1) + m_2 l(v_2)$, with nonnegative m_1 and m_2. Let z be the point $x + m_1 v_1 + m_2 v_2$. Then $d(x,z) = \rho(x)$ and $d(z,y) = (m_1 + n_1) l(v_1) + (m_2 + n_2) l(v_2) = d(y,x) + d(x,z)$. From $z \in \overline{B}(x, \rho(x)) \subseteq \overline{B}(y, \rho(y))$ it follows that $d(x,y) \leq \rho(y)$. From these relations it can be deduced that

$$\rho(y) - \rho(x) \geq d(z,y) - \rho(x) = d(z,y) - d(x,z) = d(x,y).$$

∎

This is a global criterion: in order to detect whether x is a medial axis point, all points y must be inspected. Just like in the previous section, this criterion can be reduced to a local one. All points which can be reached in a single step from x must be inspected. In the present situation, this leads to the inspection of 16 neighbors: the eight 8-neighbors and eight points which are a knights move apart from x.

13 Theorem *Let X be a bounded object in $\mathbb{Z}^2$ and let x and y be points such that $\rho(y) \geq \rho(x) + d(x,y)$. Then there is a 16-connected neighbor y' of x such that $\rho(y') \geq \rho(x) + d(x,y')$.*

PROOF. The proof is completely analogous to the proof in the previous section. If n_1, n_1, v_1, v_2 are as described in the proof of the previous theorem, it can be assumed without loss of generality that $n_1 > 0$ and the point y' can be chosen to be $x - v_1$. ∎

The second case, in which $\rho(x)$ is contained in just one of the sets $5\mathbb{N} + 11\mathbb{N}$ and $7\mathbb{N} + 11\mathbb{N}$, is more complicated. Again, our aim is to determine for each point x whether there is a point $y \neq x$ such that $\overline{B}(x, \rho(x)) \subseteq \overline{B}(y, \rho(y))$. We will not try to find a criterion which decides whether this relation holds for two arbitrary points x and y. Rather, we will show that if, for a given x, such a point y exists, there is also a point y' near x such that $\overline{B}(x, \rho(x)) \subseteq \overline{B}(y', \rho(y'))$. How near to x this point y' will be depends on the value of $\rho(x)$. It is then sufficient to check whether this neighborhood contains a point y which satisfies $\overline{B}(y, \rho(y)) \subseteq \overline{B}(x, \rho(x))$. If there is no such point, then x is a medial axis point, otherwise it is not.

Note that it depends only on $\rho(x)$, $\rho(y)$ and $x - y$ whether or not $\overline{B}(y, \rho(y)) \subseteq \overline{B}(x, \rho(x))$. For each value of $\rho(x)$, only a finite number of values for $x - y$ occurs, and for each of them there is a number $t(\rho(x), x - y)$ such that $\overline{B}(y, \rho(y)) \subseteq \overline{B}(x, \rho(x)) \Leftrightarrow \rho(y) \geq \rho(x) + t_(\rho(x), x - y)$.

As there is only a finite number of values of $\rho(x)$ for which the second case applies, and there is moreover a finite number of values of $x - y$ which are relevant, it is possible to precompute a table of all relevant values of $t_(\rho, x - y)$. Testing whether $\overline{B}(y, \rho(y)) \subseteq \overline{B}(x, \rho(x))$ is then just a matter of table look-up.

We will now examine the environments to be checked for each $\rho(x)$. In order to simplify the discussion, we will suppose that x is the origin. We divide $\mathbb{Z}^2$ in eight octants, as shown in figure 2. The octants will be called the $(2,1)$-octant, the $(1,2)$-octant, the $(-1,2)$-octant, etc., after the prime vector of type 11 they contain. Note that the symmetry group D_4, which consists of four rotations (including the identity) and four reflections in horizontal, vertical and diagonal

lines, maps a point in one octant to a point in each of the other octants. Therefore we can assume without loss of generality that y lies in the $(-1,-2)$-octant.

Suppose that z is a point in the $(1,2)$-octant. Let $z_1 = z, z_2, \ldots, z_8$ be the images under D_4 of the point z. It can easily be seen that $d(y,z_i) \leq d(y,z)$ for all i. Consequently, the sphere $\overline{B}(0,\rho(0))$ is completely contained in $\overline{B}(y,\rho(y))$ if the intersection of the sphere centered at 0 with the $(1,2)$-octant is completely contained in the sphere centered at y.

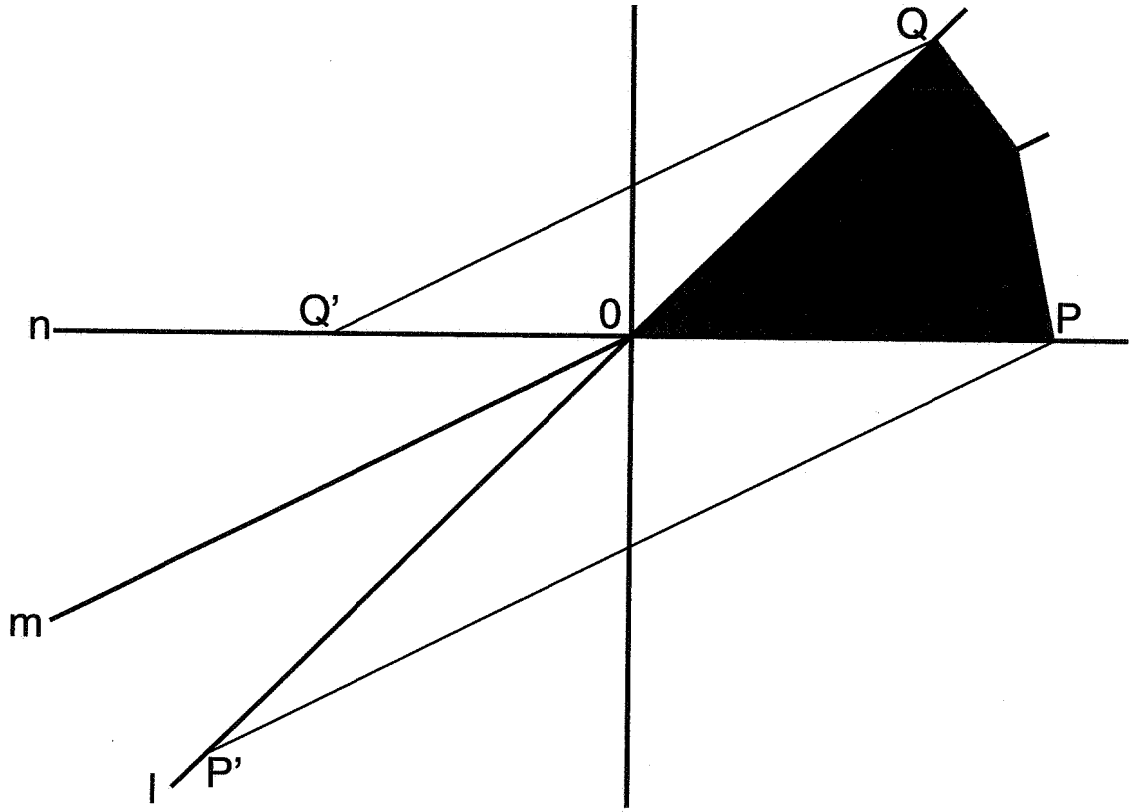

Figure 3: The geometry of the situation under consideration. See the text for an explanation.

As a consequence of the two previous paragraphs, we can restrict to the situation depicted in figure 3. Let r be an abbreviation for $\rho(0)$. Let l, m and n be the lines through the origin in the directions $(1,1)$, $(2,1)$ and $(1,0)$, respectively. Let P and Q be the points $(\lfloor r/5 \rfloor, 0)$ and $(\lfloor r/7 \rfloor, \lfloor r/7 \rfloor)$ and let $P' = (-\lfloor r/5 \rfloor, -\lfloor r/5 \rfloor)$ and $Q' = (-\lfloor r/7 \rfloor, 0)$ be their projections on the lines l and n in the $(2,1)$-direction. The shaded region represents the intersection of $\overline{B}(0,r)$ with the $(2,1)$-octant. This region will be referred to as the *opposite part* of the sphere. It lies above the line PP' and below the line QQ'.

Let y be a point in the $(-2,-1)$-octant such that $\overline{B}(0,r) \subseteq \overline{B}(y,\rho(y))$. We are now ready to construct a point y' near 0 such that $\overline{B}(0,r) \subseteq \overline{B}(y',\rho(y'))$ as well.

14 Theorem *Let y be a point in the $(-2,-1)$-octant such that $\overline{B}(0,\rho(0)) \subseteq \overline{B}(y,\rho(y))$. Then $\overline{B}(0,\rho(0)) \subseteq \overline{B}(y',\rho(y'))$ if y' satisfies the following conditions:*
(1) y' lies in the $(-2,-1)$-octant.
(2) $d(y,z) = d(y,y') + d(y',z)$ for every z in the opposite part of the sphere.

PROOF. It is sufficient to show that

$$\overline{B}(0,\rho(0)) \subseteq \overline{B}(y',\rho(y)-d(y,y')) \subseteq \overline{B}(y,\rho(y)).$$

As y' lies in the $(-2,-1)$-octant, the first inclusion can be proven by showing that $d(y',z) \leq \rho(y) - d(y,y')$ for each point z in the opposite part, i.e. for each z in the $(2,1)$-octant with $d(z,0) \leq \rho(0)$. But according to (2), we have for such points z: $d(y',z) = d(y,z) - d(y,y')$. Because $\overline{B}(0,\rho(0)) \subseteq \overline{B}(y,\rho(y))$ we know $d(y,z) \leq \rho(y)$, so $d(y',z) \leq \rho(y) - d(y,y')$.

The second inclusion holds because $d(z,y') \leq \rho(y) - d(y,y')$ implies $d(z,y) \leq d(z,y') + d(y',y) \leq \rho(y)$. ∎

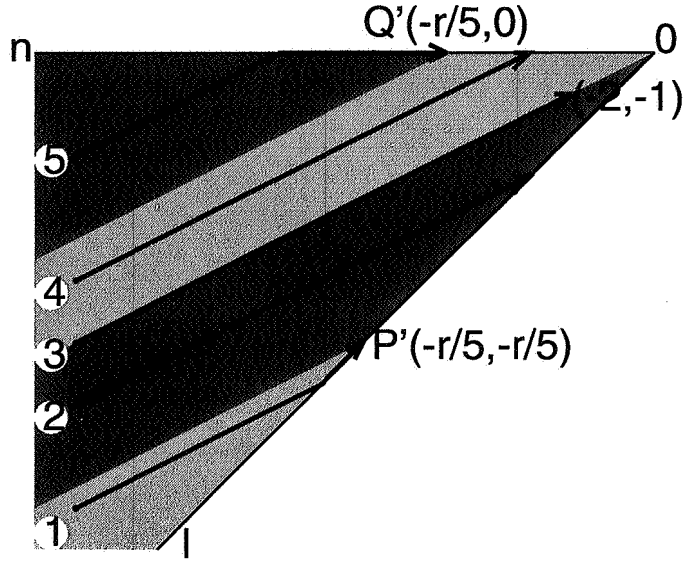

Figure 4: The construction of the points y' from the points y on the left. The points y' are found by moving in the $(2,1)$-direction until the line l or n is hit. If the line is hit to the left of P' or Q', move rightward along the line to one of these points. Regions 1, 2, 4 and 5 are the shaded areas; region 3 is the half line ending at $(-2,-1)$.

Consider again the situation of figure 3. We will construct a point y' which satisfies the conditions mentioned in theorem 14. The point y lies in one of five regions (see figure 4).

Region 1. $y = -\alpha(2,1) - \beta(1,1)$ with $\alpha \geq 0, \beta \geq \lfloor r/5 \rfloor$. Then we take $y' = P'$. Clearly, P' lies in the $(-2,-1)$-octant. We have $P' - y = \alpha(2,1) + (\beta - \lfloor r/5 \rfloor)(1,1)$, a nonnegative linear combination of $(2,1)$ and$(1,1)$. Because all points in the opposite part of the sphere lie above the line PP' and below l, it is possible for each point z in the opposite part to write $z - P'$ as a nonnegative linear combination of $(1,1)$ and $(2,1)$ as well. This implies $d(y,P') + d(P',z) = d(y,z)$.

Region 2. Suppose $y = -\alpha(2,1) - \beta(1,1)$ with $\alpha \geq 0, 0 < \beta < \lfloor r/5 \rfloor$. Then we take $y' = -\beta(1,1)$. Clearly, this y' lies in the $(-2,-1)$-octant. We have $y' - y = \alpha(2,1)$. Because the opposite part lies below the line l and above the x-axis, it is possible for all points z in the opposite part to write $z - y'$ as a nonnegative linear combination of either $(1,1)$ and $(2,1)$ or $(2,1)$ and $(1,0)$. In both cases, $d(y,y') + d(y',z) = d(y,z)$.

Region 3. Suppose $y = -\alpha(2,1)$ with $\alpha > 0$. Then we take $y' = (-2,-1)$. Clearly y' lies in the $(-2,-1)$-octant. We have $y' - y = -(\alpha - 1)(2,1)$. As the opposite part lies below the line l and above x-axis, it is possible write for each z in the opposite part to write $z - y'$ as a nonnegative linear combination of either $(1,1)$ and $(2,1)$ or $(2,1)$ and $(0,1)$. In both cases $d(y,y') + d(y',z) = d(y,z)$.

Region 4. Suppose $y = -\alpha(2,1) - \beta(1,0)$ with $\alpha \geq 0, 0 < \beta < \lfloor r/7 \rfloor$. Take $y' = -\beta(1,0)$, as we did for y in region 2.
Region 5. Suppose $y = -\alpha(2,1) - \beta(1,0)$ with $\alpha \geq 0, \beta \geq \lfloor r/7 \rfloor$. Take $y' = Q'$, as we did for y in region 1.

We have now arrived at a local neighborhood of the origin which must be inspected in order to determine if the origin is a medial axis point. This environment contains $\lfloor \rho(0)/7 \rfloor$ points in each of the four horizontal or vertical directions, $\lfloor \rho(0)/5 \rfloor$ points in each of the four diagonal directions and eight points at a knights jump from the origin. Of course, similar environments for other points can be found by translation. Note that the size of the environment depends on the value of $\rho(x)$. Figure 5 shows the environment corresponding to $\rho(0) = 31$. The environment contains horizontal and vertical branches of length $\lfloor \frac{31}{7} \rfloor = 4$, diagonal branches of length $\lfloor \frac{31}{5} \rfloor = 6$ and eight points at a knights move from the center.

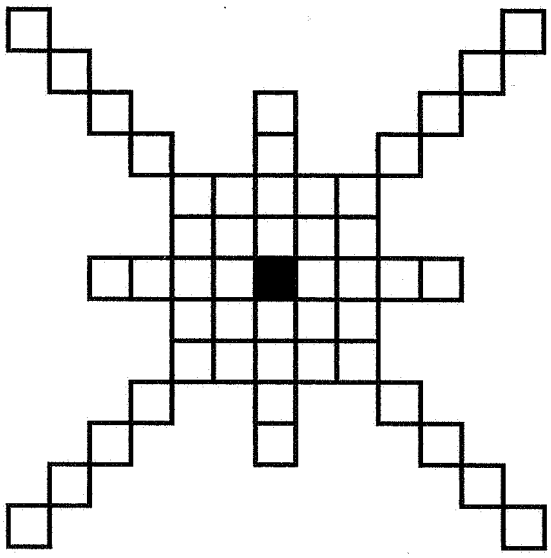

Figure 5: The neighborhood which must be investigated for a point with a distance transform value of 31.

We are now left with a finite number of internal distance transform values $\rho(x)$ for which case 2 ($\rho(x)$ in just one of the sets $5\mathbb{N} + 11\mathbb{N}$ and $7\mathbb{N} + 11\mathbb{N}$) applies, and for each of these values, with a finite environment to be inspected. The no-upstream rule does not apply in this case, but for each pair $\rho(0)$ and y we can compute (by simple trial and error) the smallest value $t(\rho(0), y)$ for which $\overline{B}(0, \rho(0)) \subseteq \overline{B}(y, t(\rho(0), y))$. These values are stored in a look-up table. When all of these values are known, we can decide whether 0 is a medial axis point by inspecting all points y in the appropriate environment and testing whether there are points y such that $\rho(y) \geq t(\rho(0), y)$. If there are such points, 0 is not a medial axis point, otherwise it is.

The discussion in this section leads to an efficient algorithm for the computation of the medial axis associated with the 5-7-11-metric. For this algorithm, some data must be computed in advance. These data are:

- The set S of all integers which are either in $5\mathbb{N} + 11\mathbb{N}$ or in $7\mathbb{N} + 11\mathbb{N}$, but not in both. This is the set $\{5, 7, 10, 14, 15, 16, 18, 20, 26, 27, 28, 29, 30, 31, 37, 38, 39, 41, 45, 48, 52, 59\}$.
- For each $r \in S$, the local environment N_r as illustrated in figure 5.
- For each point y in each environment N_r: $t(r, y)$, the smallest value t such that $\overline{B}(0, r) \subseteq \overline{B}(y, t)$.

The medial axis can be computed using the following

15 Algorithm *The computation of the medial axis of a bounded subset X of $\mathbb{Z}^2$, using the 5-7-11-metric (first version).*

(1) Computed the external distance transform of X.

(2) Compute the internal distance transform of X from the external one.

(3) For each point x in X, let r be $\rho(x)$.

- *If $r \in S$, mark x as a medial axis point if there is no $y \in N_r$ such that $\rho(x+y) \geq t(r,y)$.*
- *If $r \notin S$, mark x as a medial axis point if there is no 16-connected neighbor y of x such that $\rho(y) \geq r + d(x,y)$.*

This algorithm requires scanning a neighborhood N_r for a number of pixels. The efficiency of the algorithm can be enhanced by choosing the neighborhoods to be scanned as small as possible. The neighborhoods N_r we described are not optimal. This can be seen from an example. Consider the case $r = 10$. The point $(-2,-2)$ is an element of N_{10}, and $t(10,(-2,-2)) = 22$. A simple inspection (see figure 6) shows that

$$\overline{B}((0,0),10) \subseteq \overline{B}((-1,-1),16) \subseteq \overline{B}((-2,-2),22).$$

Consequently, if $\rho(0) = 10$ and $(-2,-2)$ is a point y such that $\overline{B}(0,10) \subseteq \overline{B}(y,\rho(y))$, then so is $(-1,-1)$. This implies the the point $(-2,-2)$ does not have to be checked for the case $\rho(0) = 10$: if $(0,0)$ is rejected as a medial axis point because $\overline{B}((0,0),10) \subseteq \overline{B}((-2,-2),\rho((-2,-2)))$, then it will also be rejected as a medial axis point because $\overline{B}((0,0),10) \subseteq \overline{B}((-1,-1),\rho((-1,-1)))$.

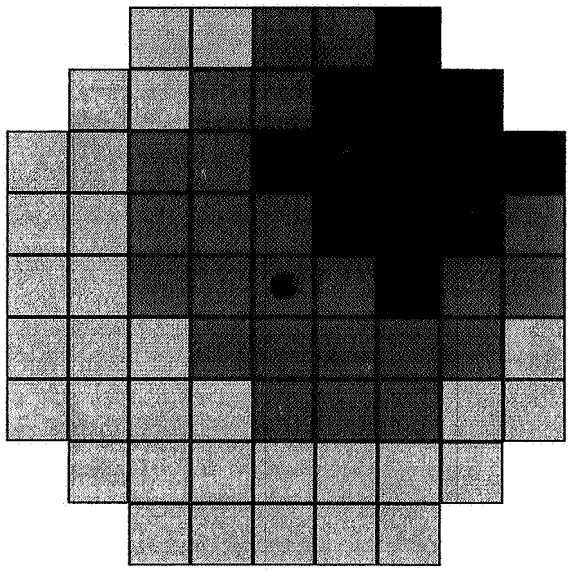

Figure 6: Three nested spheres having radii 10, 16 and 22 and centers $(0,0)$, $(-1,-1)$ and $(-2,-2)$.

As the number of values of $\rho(0)$ for which a larger neighborhood must be inspected is finite, it is possible to investigate all cases and to remove as much points from the environments as possible. This produces reduced environments $\hat{N}_r$. In the case of the 5-7-11-metric, each reduced environment appears to be the set of 16-connected neighbors. The author believes that this is typical for the 5-7-11-metric, but not true for all p-q-r-metrics.

The numbers $t(r,y)$ also happen to have a nice characterization in the case of the 5-7-11-metric. It appears that

$$t(r,y) = \begin{cases} d(y,0)-1 & \text{if } y \text{ is a type-5 vector and } r \notin 5\mathbb{N}+11\mathbb{N} \\ & \text{or } y \text{ is a type-7 vector and } r \notin 7\mathbb{N}+11\mathbb{N} \\ d(y,0) & \text{otherwise} \end{cases}$$

The author has examined the p-q-r-metrics with $r \leq 50$, and it appears that a sixteen pixels neighborhood is sufficiently large for all values of $\rho(0)$, for all of these metrics. Moreover, the characterization of $t(r,y)$ described above appears to hold for all of these metrics. The author has not been able to prove a general result, though.

The observation made in this section lead to a more efficient version of the medial axis algorithm. The algorithm uses three variables T_5, T_7 and T_{11}, which correspond to values of $t(\rho(0),y)$ for vectors y of type 5, 7 and 11, respectively. If x is a vector of type 5, 7 or 11, then T_x denotes T_5, T_7 or T_{11}, respectively.

16 Algorithm *The computation of the medial axis of a bounded subset X of $\mathbb{Z}^2$, using the 5-7-11-metric (second version).*

(1) Compute the external distance transform of X.
(2) Compute the internal distance transform ρ of X from the external one.
(3) For all points $x \in X$:
- *Set the type 11 step size T_{11} to 11.*
- *If $\rho(x) \notin 5\mathbb{N}+11\mathbb{N}$, set the type-5 step size T_5 to 4, otherwise set T_5 to 5.*
- *If $\rho(x) \notin 7\mathbb{N}+11\mathbb{N}$, set the type 7 step size T_7 to 6, otherwise set T_7 to 7.*
- *Mark x as a medial axis point if there is no 16-neighbor y of x such that $\rho(y) = \rho(x)+T_{y-x}$.*

5. The Opening Transform and the Pattern Spectrum

In this section, we present the opening transform and the pattern spectrum, and an efficient algorithm for their computation, based on the medial axis. An operator α mapping subsets of a set E to subsets of E is called an *opening* [13] if it satisfies the following properties for each $X, Y \subseteq E$:
(1) $X \subseteq Y \rightarrow \alpha(X) \subseteq \alpha(Y)$.
(2) $\alpha(\alpha(X)) = \alpha(X)$.
(3) $\alpha(X) \subseteq X$.

From now on, we will restrict to the openings on the square grid $\mathbb{Z}^2$ and we will assume that this grid is provided with a chamfer metric. The most common opening is the *structural opening*, which can be constructed by "filling" a set with translates of a structuring elements: $X \circ A = \bigcup\{A_h \mid h \in E, \quad A_h \subseteq X\}$. The structural opening $X \circ \overline{B}(r)$ of a set X with a sphere of radius $r \in D$ is

$$X \circ \overline{B}(r) = \bigcup\{\overline{B}(x,r) \mid x \in \mathbb{Z}^2, \overline{B}(x,r) \subseteq X\}.$$

A *granulometry* or *size distribution* [6, 7] is defined as a family $\{\alpha_r\}$ of openings, where the range of r is some ordered set and

$$\alpha_r \alpha_s(X) = \alpha_{\max(r,s)}(X).$$

In this paper, the range of r will be D. The family of structural openings with discs of a given radius is not a size distribution, but it is possible to construct a size distribution $\{\alpha_r\}_{r \in D}$ from them by

$$\alpha_r(X) = \bigcup_{s \geq r} X \circ \overline{B}(s).$$

From the definition of a size distribution, it follows that $x \in \alpha_r(X) \Rightarrow x \in \alpha_s(X)$ for all $s \leq r$. This observation is the inspiration for the definition of the opening transform.

17 Definition *Let X be a bounded subset of $\mathbb{Z}^2$ and let $\{\alpha_r\}$ be a size distribution. The opening transform A_X is the mapping from X to D defined by*

$$A_X(x) = \max\{r \in D \mid x \in \alpha_r(X)\}.$$

Important information on the shape of X can be obtained by monitoring the change of $\alpha_r(X)$ as the parameter r is varied. Maragos [6] defines the pattern spectrum (for subsets of $\mathbb{R}^2$, provided with the Euclidean metric) as

$$p_X(r) = \frac{\mathrm{d}A(X \circ B(r))}{\mathrm{d}r},$$

where $A(X \circ B(r))$ is the area of $(X \circ B(r)$. For the discrete case, this produces the following

18 Definition *[6] Let X be a bounded subset of $\mathbb{Z}^2$ and let α_r be the size distribution induced by a chamfer metric d. The the pattern spectrum $p(r)$ is the function from D to $\mathbb{N}$ defined by*

$$p_X(r) = |\alpha_r(X)| - |\alpha_{r^+}(X)|,$$

where $|\cdot|$ denotes the number of points in a set and $r^+ = \min\{r' \in D \mid r' > r\}$ is the smallest element of D which is larger than r.

Note that the pattern spectrum of a set is equal to the histogram of its opening transform. It is therefore possible to compute the pattern spectrum directly from the opening transform. In the rest of this section, we will therefore discuss only the opening transform.

From the definitions of A_X and α_r it follows that

$$A_X(x) = \max\{r \in D \mid x \in \overline{B}(y, r) \subseteq X \text{ for some } y \in \mathbb{Z}^2\}.$$

Because for each $x \in X$, the largest disc centered at x and contained in X has radius $\rho(x)$, this can be reduced to

$$A_X(x) = \max\{\rho(y) \mid y \in \mathbb{Z}^2, x \in \overline{B}(y, \rho(y))\}.$$

Observe that for each x and y such that $x \in \overline{B}(y, \rho(y))$, there is also a point m in the medial axis M_X such that $x \in \overline{B}(m, \rho(m))$. This leads to the relation

$$A_X(x) = \max\{\rho(m) \mid m \in M_X, x \in \overline{B}(m, \rho(m))\}.$$

This relation can be used to compute the opening transform by successively inspecting all maximal spheres in a bounded object X. First, all pixels in the result image are given value zero. The medial axis is computed, and each medial axis point is inspected in turn. If m is the medial axis point being inspected, then all pixels in the sphere $\overline{B}(m, \rho(m))$ in the result image are visited. If the present value if the pixel in the result image is smaller than $\rho(m)$, the value is updated to $\rho(m)$. In the algorithm presented here, the medial axis points are sorted in order of increasing distance transform value and visited in this order. Thus, when the points in $\overline{B}(m, \rho(m))$ are being visited, a pixel in the result image can never have a value larger that $\rho(m)$, and the pixels in $\overline{B}(m, \rho(m))$ can always be assigned value $\rho(m)$, without prior inspection of the present pixel value. This strategy enhances the efficiency of the algorithm, because a comparison of pixel values in the inner loop is replaced by a sorting of the medial axis points, which must be performed just once. As $\rho(m)$ assumes only integer values smaller than some maximal value, the medial axis points can be sorted in linear time in the number of medial axis points using distribution sorting [5].

The efficiency of the algorithm depends on an efficient way of addressing all pixels in a sphere $\overline{B}(m, \rho(m))$. Certainly, computing such spheres in a two scan reconstruction algorithm would be too costly. In stead, the pixels in the sphere $\overline{B}(0, R)$, where R is the largest occurring value of $\rho(m)$, are sorted in order of increasing distance to the origin. When the sorted list is computed, the pixels in each sphere $\overline{B}(0, r)$ for $r \leq R$ can be found by taking a suitable first part of the list. The pixels in spheres with different centers can be found by translation. In practice, the pixels in $\overline{B}(0, R)$ are not sorted, but computed in the correct order, and pixel positions are represented as relative offsets in the image array in order to provide fast access to the image.

Summarizing, the opening transform can be computed by the following

19 Algorithm *The computation of the opening transform of a bounded subset X of $\mathbb{Z}^2$ according to some chamfer metric d.*

(1) Initialize the result image to 0.
(2) Compute the distance transforms ρ_X^{ext} and ρ and the medial axis M_X.
(3) Sort the medial axis points in order of increasing distance transform value.
(3) For all medial axis points, in increasing order:
- *Set the pixels in $\overline{B}(m, \rho(m))$ to $\rho(m)$.*

As noted before, the size distribution of X is the histogram of A_X, so it can be computed from A_X in a very straightforward way.

Figure 7 shows a binary image, its medial axis and its distance transform. Dark pixels correspond to large distance transform values. The computation of the opening transform took 0.43s, which is two orders of magnitude faster that the 45s required by the brute force algorithm described in [10]. A similar reduction of computation time is found for other images.

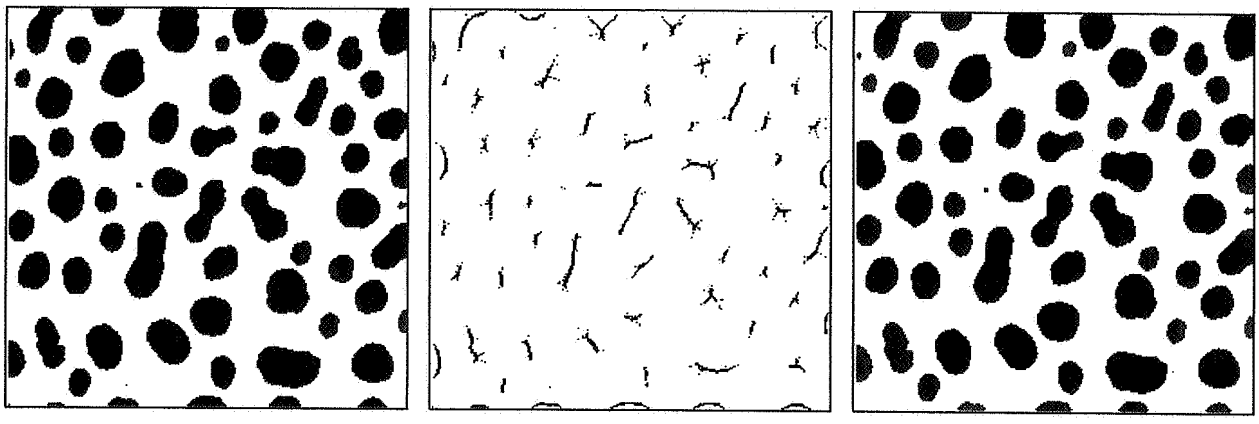

Figure 7: A binary image, its medial axis and its opening transform as defined by the 5-7-11 metric.

6. Conclusions

In this paper, we presented a method for computing the medial axis defined by spheres in the 5-7-11-chamfer metric. This result is an extension of the results in a previous paper [10], where an algorithm for the class of extending metrics was presented. The method is based an the understanding of the structure of shortest paths in the 5-7-11 metric and of the structure of its range.

The 5-7-11- metric approximates the Euclidean distance with an accuracy of 1.79%, which is sufficient in most practical cases. The method proposed here produces a close approximation to

the Euclidean medial axis. Yet the algorithm is very efficient, requiring only four image scans, and local computation in each scan.

In the medial axis algorithm, it is necessary to scan for each pixel x an environment whose size depends on the value $\rho(x)$ of the internal distance transform. It has been shown how the efficiency of the algorithm can be further improved by reducing the size of the neighborhoods which are investigated for each pixel. Investigation of the p-q-r-metrics with $r \leq 50$ has shown that a neighborhood of 16 pixels is sufficient for all values of $\rho(x)$ and for all of these metrics. Whether or not such an environment suffices for all p-q-r-metrics remains an open problem.

Based on the medial axis transform, we presented an algorithm for the computation of the opening transform and the pattern spectrum associated with the 5-7-11 metric. The algorithm also uses a smart addressing scheme for pixels within a sphere of given center and radius. The approach based on the medial axis is two orders of magnitude faster than a brute force algorithm.

Acknowledgements

The author thanks H. Heijmans, F. Groen and A. Toet for their discussions on contents and form of the manuscript.

[1] C. Arcelli and G. Sanniti di Baja. Finding local maxima in a pseudo-euclidean distance transform. *Computer Vision, Graphics and Image Processing*, 43:361–367, 1988.

[2] G. Borgefors. Distance transformations in arbitrary dimensions. *Computer Vision, Graphics and Image Processing*, 27:321–345, 1984.

[3] L. Dorst. Pseudo-euclidean skeletons. In *Proceedings of the Eighth International Conference on Pattern Recognition*, 1989.

[4] H. Heijmans and C. Ronse. The algebraic basis of mathematcial morphology part 1: Dilations and erosions. *Computer Vision, Graphics and Image Processing*, 50:245–295, 1990.

[5] D. Knuth. *The Art of Computer Programming Volume 3: Sorting and Searching.* Addison-Wesley, Reading Mass., U.S.A., 1973.

[6] P. Maragos. Pattern spectrum and multiscale shape representation. *IEEE Transactions on Pattern Analysis and Machine Intelligence*, 11(7):701–715, 1989.

[7] G. Matheron. *Random Sets and Integral Geometry.* Wiley, New York, 1975.

[8] G. Matheron. Examples of topological properties of skeletons. In J. Serra, editor, *Image Analysis and Mathematical Morphology Volume 2: Theoretical Advances.* Academic Press, London, 1988.

[9] F. Meyer. Skeletons and perceptual graphs. *Signal Processing*, 16:335–363, 1989.

[10] P. F. Nacken. Chamfer metrics in mathematical morphology. (to be published).

[11] C. Niblack, D. Capson, and P. Gibbobs. Generating skeletons and centerlines from the medial axis transform. In *Proceedings of the Tenth International Conference on Pattern Recognition*, 1990.

[12] C. Ronse and H. Heijmans. The algebraic basis of mathematical morphology part 2: Openings and closings. *CVGIP Image Understanding*, 54(1):74–97, 1991.

[13] J. Serra. *Image Analysis and Mathematical Morphology.* Academic Press, London, 1982.

[14] B. Verwer. Local distances for distance transformations in two and three dimensions. *Pattern Recognition Letters*, 12(11):671–682, 1991.